J. Electroanal. Chem., 308 (1991) 295–307
Elsevier Sequoia S.A., Lausanne

The structure of halide adlayers on Ag (111) electrodes

M.S. Zei

Fritz-Haber-Institut der Max-Planck-Gesellschaft, Faradayweg 4–6, W-1000 Berlin 33 (Germany)

(Received 10 September 1990; in revised form 2 January 1991)

Abstract

The structure of chloride and bromide adlayers on Ag (111) electrodes has been studied by LEED, RHEED and AES as a function of the emersion potential. No ordered halide adsorption could be found in the potential range negative of about −0.2 V (vs. SCE), whereas a hexagonal ordered adlayer (1.38 × 1.38) of Cl and a local ($\sqrt{3} \times \sqrt{3}$)R30°-Br structure were observed after emersion from NaCl and NaBr solutions, respectively, at a potential of around +0.1 V.

INTRODUCTION

The adsorption of halide ions on silver crystal surfaces has been the subject of a number of papers [1–3] in which the phenomenon has been studied mostly by means of voltammetric and capacitative experiments. However, the structure determination of the halide adlayer for an emersed electrode has rarely been reported, except for a recent publication by Salaita et al. [4] concerning the structure of the halide overlayer on an Ag (111) surface. They found a ($\sqrt{3} \times \sqrt{3}$)R30° structure after emersion from chloride and bromide solutions at a potential around +0.1 V.

In the present work, the structure of the halide adlayer as a function of the emersion potential has been studied by LEED, RHEED, AES and voltammetry. In addition to our interest in the correlation between the voltammetric peak and the adlayer structure on the Ag (111) electrode surface in chloride and bromide solutions, we have found a remarkable similarity between Cl liquid phase and gas phase adsorption on Ag (111) which was carried out under UHV conditions [5]. Both systems show that Cl adatoms form a random layer at low Cl coverage with an Auger intensity ratio (I_{Cl}/I_{Ag}) less than 0.4, i.e. the electrode emersion potential is below +0.1 V, but an ordered layer (1.38 × 1.38) at higher coverage for the Ag electrode emersed at a potential around +0.15 V. These results may provide an interesting aspect concerning the Cl catalytic promotion of ethylene oxidation with respect to the two Cl adlayer phases, which may exist on the Ag (111) catalyst

0022-0728/91/$03.50

surface during oxidation reactions. Moreover, the formation of an ordered overlayer of Br on the Ag (111) surface occurs only in the positive potential range, around +0.1 V; a $(\sqrt{3} \times \sqrt{3})$R30°-antiphase domain structure is observed in the NaBr electrolyte. At very negative potentials ($V = -1.0$ V), no ordered halide overlayer can be observed except for the salt crystals (NaCl, NaBr) due to wet emersion.

EXPERIMENTAL

The apparatus has been described in previous papers [6,7]. In the LEED experiment, the electrons impinge perpendicularly to the sample surface as shown in Fig. 1a. LEED images a two-dimensional reciprocal lattice. The arrangement of the

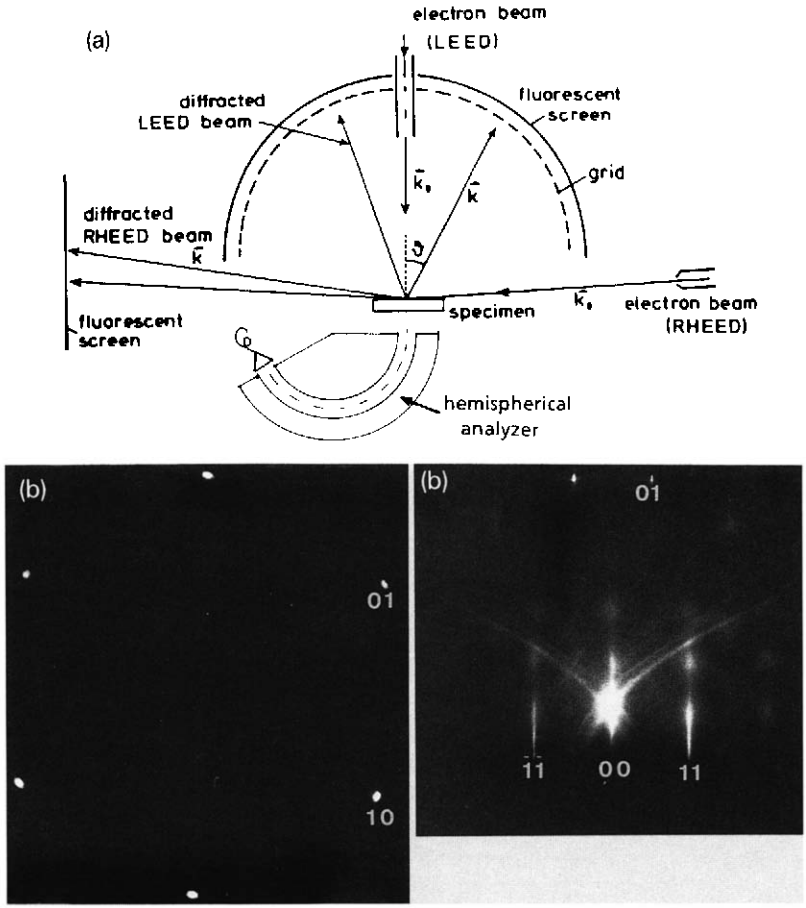

Fig. 1. (a) Experimental set-up for surface studies by LEED, AES and RHEED. k_0 and k are the wave vectors of incoming and diffracted beams, respectively. (b) LEED (62 eV) and RHEED (⟨112⟩) patterns of an Ag (111) electrode after Ar^+ bombardment and annealing at ca. 500 °C.

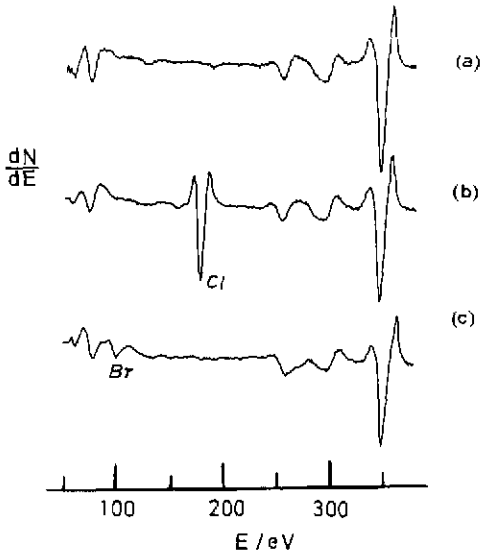

Fig. 2. Auger spectra of an Ag (111) electrode (a) after preparation in a UHV chamber (b) after cycling in 0.01 M NaCl between −1.0 and 0.2 V and emersion at +0.16 V, and (c) after cycling in 0.01 M NaBr between −1.0 and +0.2 V and emersion at 0.05 V.

adsorbate with respect to the substrate surface can be deduced conveniently from the pattern. On the other hand, RHEED (reflection high energy electron diffraction) was performed with electrons of 40 keV energy at grazing angles of 1–2° (see Fig. 1a). Although a RHEED pattern shows only a one-dimensional reciprocal lattice row perpendicular to the direction of the incident electron beam, it has a higher resolution compared with LEED in the geometrical relation in the reciprocal space. In addition, the RHEED gun can also be used for AES measurements, as shown in the schematic set-up in Fig. 1a. For the AES experiment the sample has to be rotated by 180° from the position shown in Fig. 1a in order for the sample to face the entrance slit of the 150° hemispherical analyser. For AES experiments we can use both AES and RHEED guns at angles of grazing incidence. In the present work, we used mainly the RHEED gun, because we could observe the RHEED pattern during the AES measurements which are then correlated directly to the RHEED pattern from the adsorbate.

The surface of the Ag (111) single crystal was prepared by cycles of argon ion bombardment (5×10^{-5} Torr, 1 h) and annealing (500–600 °C) by resistance heating in a UHV chamber. After cleaning and annealing, the Ag surface was characterized by LEED, RHEED (Fig. 1b) and Auger spectroscopy (Fig. 2). The specimen was transferred by means of a set of mechanically and magnetically coupled manipulators into an electrochemical chamber, where the electrolyte could be brought into contact with the specimen after the chamber had been backfilled with 5 N argon gas. The reference electrode was $Ag/AgCl/KCl_{(sat)}$. The electrolytes of 0.01 M

NaCl and 0.01 M NaBr were made with pyrolytic water and suprapure chemicals (E. Merck). They were deaerated with purified nitrogen gas during the cyclic voltammetry. The emersed electrode at defined electrode potentials was not rinsed with water. After evacuation of the Ar gas in the electrochemical chamber (taking ca. 10 min), the electrode was transferred back into the UHV chamber, where the electrode could again be investigated by LEED, RHEED and Auger spectroscopy.

RESULTS

Ag (111) in chloride solution

The current–potential curve for an Ag (111) electrode in 0.01 M NaCl solution shows a broad adsorption peak around -0.7 V with a spike at 0 V (Fig. 3a). The LEED patterns show a (1×1) structure with a diffuse background for the electrode which was emersed from the chloride solution at three different potentials of -1.0, -0.83 and -0.52 V. However, the RHEED patterns (Fig. 4a) for the Ag (111) electrode emersed at a potential around -0.8 V show an additional reflection streak

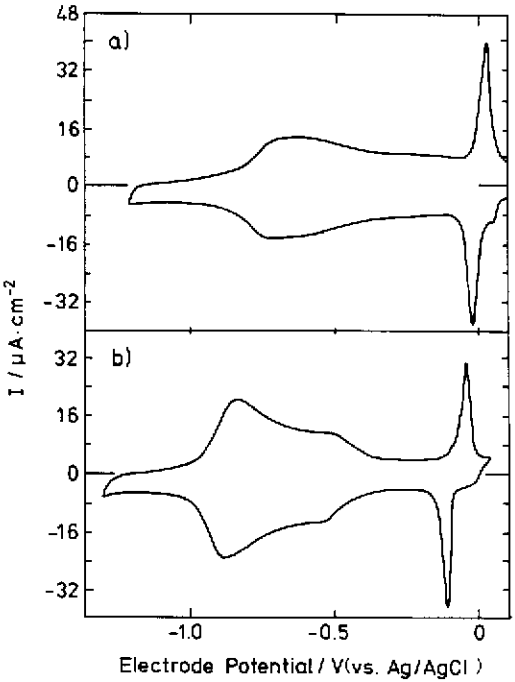

Fig. 3. Cyclic voltammetry of an Ag (111) electrode in (a) 0.01 M NaCl and (b) 0.01 M NaBr solutions. Scan rate = 100 mV/s.

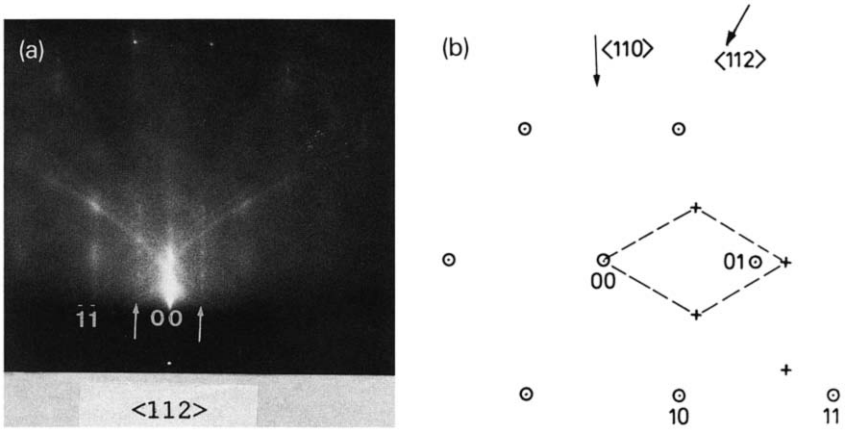

Fig. 4. (a) RHEED pattern of an Ag (111) electrode at ⟨112⟩ azimuth, after cycling in 0.01 M NaCl between −1.0 and +0.2 V and emersion at −1.0 V; the pattern shows additional reflections due to NaCl crystallites indicated by the arrows. (b) Reciprocal lattice unit cells of Ag (111) substrate (⊙) and of the epitaxial layer of NaCl (+).

with strong intensity modulation which obviously results from the three-dimensional NaCl crystals formed from the bulk electrolyte due to wet emersion. The formation of NaCl salt is confirmed by Auger spectroscopy, which shows clearly Na and Cl peaks, and by the RHEED patterns; the locations of the extra reflections in the RHEED patterns at ⟨110⟩ and ⟨112⟩ azimuths indicate the relative orientations of NaCl on the Ag (111) surface. The NaCl (111) plane is parallel to the Ag (111) surface, but with the ⟨112⟩ direction parallel to the ⟨110⟩ direction of the Ag (111) as shown in Fig. 4b, i.e. the hexagonal unit cell of the NaCl (111) layer is rotated by 30° with respect to the unit cell of the substrate surface. The potential range for observation of the salt lies approximately between −1.0 and −0.2 V. The missing LEED spots for the NaCl crystal may be explained by the fact that salt crystallization from the bulk electrolyte is not uniformly distributed over the emersed Ag electrode surface. This has also been found for hydronium perchlorate crystallization on an Au (111) surface from $HClO_4$ solution and has been confirmed by scanning electron microscopic imaging of the crystallites [8]. Thus, the LEED intensity scattered from a few crystal surfaces of the salt may be too weak to be observed, whereas the whole volume of the salt crystals contributes to the RHEED reflection intensity. Moreover, the transfer width [9] of the RHEED system is about four times larger than that of LEED in our equipment, which is another reason why the reflection seen in RHEED could not be detected by LEED.

With a more positive emersion potential of the electrode, around 0.1 V, superstructure reflections were seen in RHEED at ⟨110⟩ and ⟨112⟩ azimuths (Fig. 5a) which differ clearly from the patterns of the NaCl structure. The extra diffraction streaks indicated by the arrows in the RHEED patterns for ⟨110⟩ and ⟨112⟩ azimuths (Fig. 5a), designating the reciprocal lattice points b10 and b11 respectively,

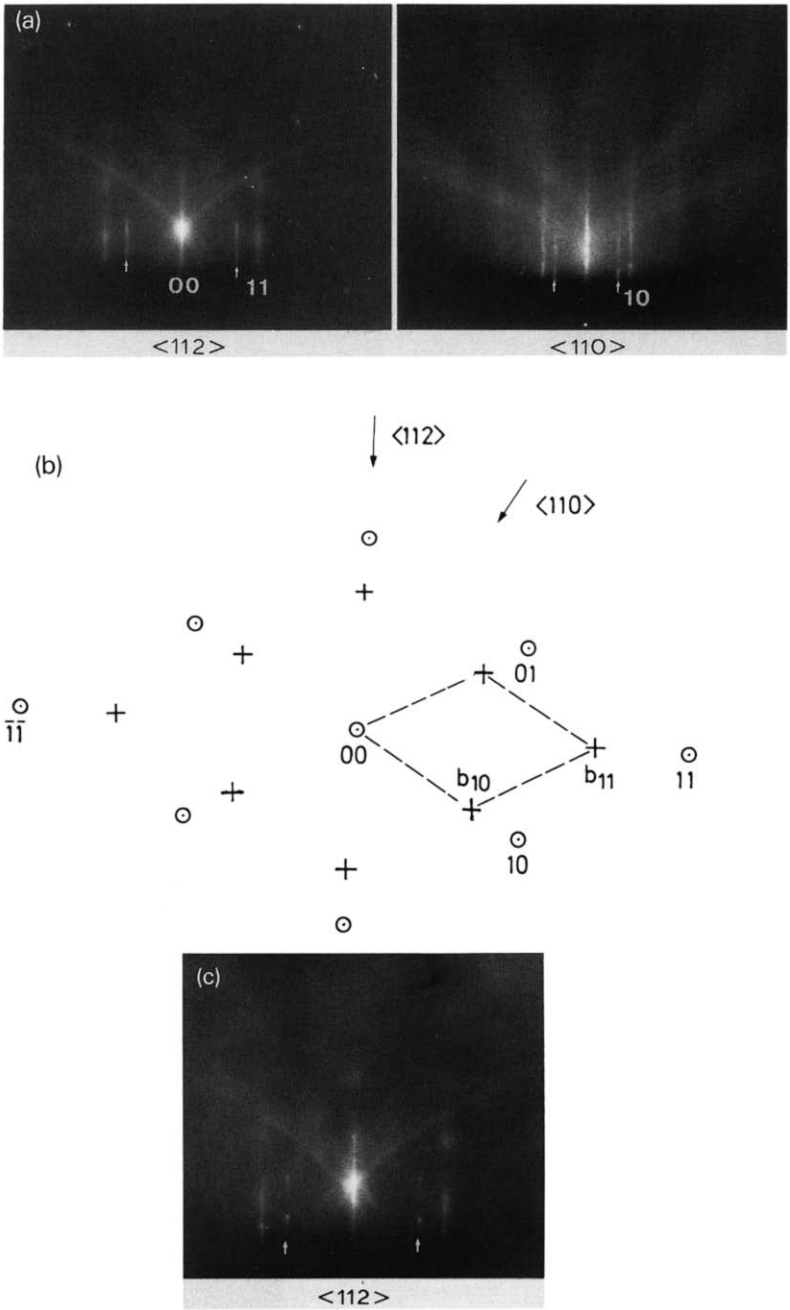

Fig. 5. (a) RHEED patterns of an Ag (111) electrode after cycling in 0.01 M NaCl between −1.0 and +0.2 V and emersion at +0.17 V, showing the Cl adlayer structure (indicated by arrows). (b) Reciprocal lattice unit cells of the Ag substrate (⊙) and of the Cl adlayer (+). (c) RHEED pattern of a three-dimensional AgCl crystallite formed locally on the Ag (111) surface. The reflections due to AgCl are indicated by arrows.

are shown in Fig. 5b. The locations of the extra reflections in Fig. 5b show that the superstructure due to Cl adsorption has a hexagonal unit mesh like the Ag (111) substrate, and the ⟨110⟩, ⟨112⟩ Cl layer directions lie along ⟨110⟩ and ⟨112⟩ of the Ag (111) substrate, respectively, i.e. the unit cell of the Cl adlayer is parallel to the substrate unit cell. The inter-row spacing of the ⟨110⟩ Cl rows deduced from the reciprocal lattice vector b10 in Fig. 5b is 3.45 Å (1 Å = 10^{-10} m), which gives an interatomic distance ($r_{\mathrm{Cl-Cl}}$) of 3.98 Å. The Cl superstructure reflection in Fig. 5a, showing a streak-form perpendicular to the shadow edge, indicates that the Cl adatoms form a two-dimensional layer structure. Here we want to emphasize that no additional reflection due to NaCl salt can be seen in Fig. 5a (cf. Fig. 4a). However, when the specimen position is moved laterally with respect to the direction of the electron incidence, three-dimensional reflection spots can occasionally be observed at certain positions of the Ag electrode surface (10–15%) as shown in Fig. 5c. The reflection spots are indicated by arrows. The reciprocal value of the distance between the three-dimensional spots perpendicular to the shadow edge gives an interlayer spacing of 3.35 Å, which is much larger than that of the Ag (111) substrate ($d111 = 2.36$ Å), but is very close to the interlayer spacing of bulk AgCl (111) (3.25 Å), which is itself a layer structure with alternating Ag and Cl layers. We conclude that these reflections reveal the existence of several layers of AgCl formed epitaxially on the Ag (111) surface. This view is confirmed by the good agreement of the lateral interatomic distance of 3.98 Å obtained from Fig. 5a with that of bulk AgCl (111) (3.93 Å). Hence the conclusion can be drawn that the AgCl (111) layers are formed due to the chemisorbed Cl atoms on a local part of the Ag electrode surface (10–15%). This three-dimensional AgCl growth observed only locally from the emersed electrodes is apparently initiated by the aggressive Cl adsorption on a defect of the electrode surface. However, the AgCl crystallites grow coincidently with respect to the Ag substrate; their unit cell is rotated by 30° with respect to the NaCl unit cell. It is interesting to note that no difference in magnitude of the reciprocal lattice vector b11 can be detected from either RHEED patterns of Figs. 5a and 5c. This means that the laterally interatomic distance of the Cl adlayer with the (1.38 × 1.38) structure is exactly the same as that in the crystalline AgCl (111) structure, i.e. it is possible that the topmost layer of the Ag electrode rearranges with

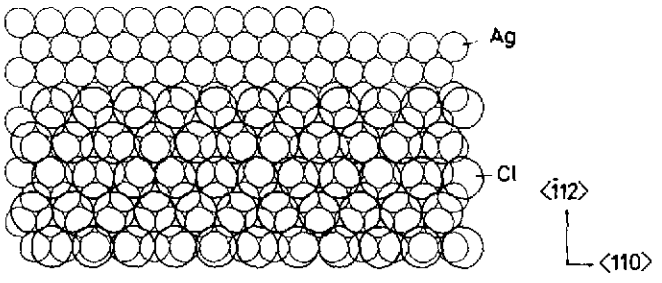

Fig. 6. Model of the Cl overlayer structure (1.38 × 1.38).

the Cl adatoms into an AgCl layer. This result is similar to the results obtained by Tu and Blakely [11] for gas phase Cl adsorption on Ag (111) under UHV conditions. They found a LEED pattern like the one shown in Fig. 5b and concluded that an AgCl (111) layer is formed epitaxially on the Ag (111) surface; this was confirmed by measurement of the heat of Cl adsorption, consistent with the heat of AgCl formation [11]. The model of the Cl adlayer structure derived from the observed RHEED patterns (Fig. 5) is given in Fig. 6, which can be interpreted as a compact pseudohexagonal overlayer.

Ag (111) in bromide solution

The current–potential curve of Ag (111) in 0.01 M NaBr solution is given in Fig. 3b, which shows a peak at around 0 V. The LEED patterns for the Ag (111) electrodes emersed at five different potentials of -1.0, -0.8, -0.6, -0.16 and 0 V show only a (1×1) structure like those reported by Salaita et al. [4], who observed a (1×1) structure for an emersed Ag (111) electrode in the same potential range in aqueous bromide solutions and claimed to see a $(\sqrt{3} \times \sqrt{3})$R30°-Br structure for the emersed electrode at potentials between 0.0 and $+0.1$ V, although the superstructure pattern was not shown. In the present paper, the RHEED patterns for the emersed Ag electrode at -1.0 V show an additional reflection appearing besides the substrate reflections in the ⟨110⟩ and ⟨112⟩ azimuths (Fig. 7), which is obviously due to the NaBr crystal formed on the Ag (111) electrode surface as a result of wet emersion. This indicates that the Ag (111) surface exhibits hydrophilic behaviour in the bromide solution, as in NaCl solution, and that the NaBr (111) crystallites grow epitaxially on the Ag (111) substrate similar to the NaCl (111) layer, i.e. the hexagonal unit cell of NaBr (111) is rotated by 30° with respect to the substrate unit cell.

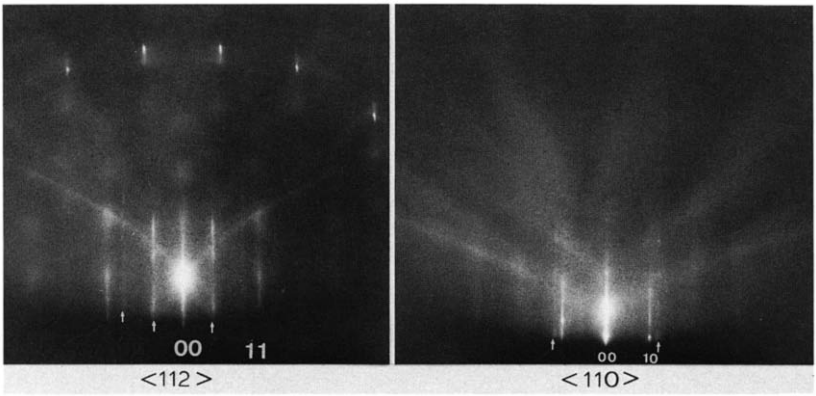

Fig. 7. RHEED pattern for an Ag (111) electrode after cycling in 0.01 M NaBr between -1.0 and $+0.2$ V and emersion at -1.0 V, showing additional reflections due to the NaBr adlayer (indicated by arrows).

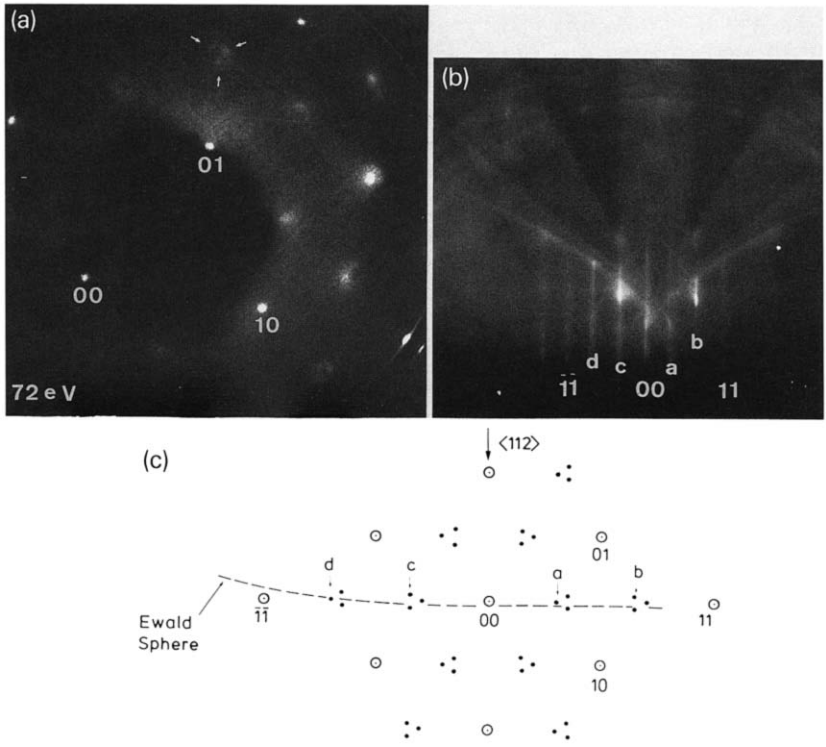

Fig. 8. (a) LEED and (b) RHEED patterns for an Ag (111) electrode after cycling in 0.01 M NaBr between −1.0 and +0.2 V and emersion at +0.03 V, showing additional reflections with splitting. (c) Reciprocal lattice unit cells of the Ag substrate (⊙) and of the Br adlayer (•) which shows splitting of the fractional-order spots.

With the electrode emersed at ca. 0.1 V, the LEED pattern in Fig. 8a shows a superstructure with triangular splitting of the fractional-order beams (n/3, n/3) as indicated by the arrows; the substrate reflection beams remain sharp as before and show no splitting. A schematic pattern of the observed reciprocal unit cell of the Ag (111) substrate (○) with splitting of the fractional-order spots (○) is shown in Fig. 8c. The splitting of the fractional-order beams can also be detected by slight rotation of the Ag crystal in the RHEED patterns (Fig. 8b), where the reflection streaks indicated by a, b, c and d are the corresponding triangular splitting spots shown in Fig. 8c.

DISCUSSION

The anodic peak of the voltammogram shown in Fig. 3a is spread over the potential range between −0.9 and −0.1 V, which may reflect the fact that the Cl adatoms are randomly adsorbed on the Ag (111) surface. After the positive scan

through the sharp peak at 0 V, they seem to rearrange into an ordered Cl overlayer, as shown in the RHEED patterns in Fig. 5. Thus, the anodic peak around 0.0 V may represent a phase transition of the Cl adlayer from an amorphous to an ordered structure. The Cl coverage deduced from the model shown in Fig. 6 is about 0.5, which agrees well with the coverage estimated from the coulometric determination of the curve in Fig. 3a which may include +15% error due to the local three-dimensional AgCl crystallite formation on the Ag electrode surface as mentioned before. This suggests that the electrosorption valency of the Cl ion is approximately close to 1.

The Auger intensity ratio of Cl to Ag (I_{Cl}/I_{Ag}) for the Ag electrode emersed at +0.17 V from the chloride solution is about 0.4, which corresponds qualitatively to a Cl coverage of ≈ 0.5 according to the AES estimation by Salaita et al. [4] from an emersed Ag electrode at the same potential. No reflection due to NaCl salt could be detected by RHEED during the AES measurements, i.e. the measured Auger signal for Cl had no contribution from NaCl.

When the Auger intensity ratio (I_{Cl}/I_{Ag}) of the gas phase Cl adsorption on Ag (111) under UHV conditions [5] was close to 0.4, LEED showed a similar pattern to that shown in the schematic diagram of Fig. 5b. There are some similarities between gas-phase and liquid-phase Cl adsorption on Ag (111) at this Cl coverage ($I_{Cl}/I_{Ag} = 0.4$); under UHV conditions, coverage approaching this value results in a well-defined LEED pattern, as shown schematically in Fig. 5b, while at lower Cl coverages, the LEED patterns show only a (1×1) structure with a diffuse background as in the liquid phase. Hence the structure of the Cl adlayer on the Ag (111) surface formed from gas phase adsorption [5,10,11] is similar to that obtained from the electrolyte, except for a slightly smaller (3%) interatomic distance. Moreover, the UPS spectra of the former case [5] show clearly additional binding energy peaks due to the strong interaction of the Ag d shell with the Cl $4p$ orbitals [12,13], indicating that there is a significant alteration in the electronic structure which may arise from bond formation of the Cl adlayer with the substrate, forming an AgCl layer. This has also been confirmed by the work of Sesselmann and Chuang [14], who used XPS, AES and Auger depth profiling techniques. Thus, the AgCl layer formation due to the Cl adsorption in the liquid phase cannot be excluded, as supported by comparison of the reciprocal lattice b11 of the RHEED patterns in Figs. 5a and 5c. This conclusion can be reached by RHEED, but not by LEED alone. The AgCl (111) layer formation is obviously accompanied by displacements of the Ag surface atoms which may cause surface roughening, as confirmed by the RHEED pattern in Fig. 5c, which shows clearly an intensity modulation along the substrate reflection streaks of (00), (11) beams. The roughening process can result in a number of small clusters on the Ag (111) surface which may be especially active for the catalytic reactions. Although there have been a number of studies on the AgCl/Cl system [15,16] which are useful for understanding the promotion effect of the adsorbed chlorine on the Ag catalyst surface during ethylene oxidation, an explanation for the Cl promotion mechanism has not yet been established. The present results from a well-characterized single-crystal surface show that there are two Cl adlayer phases

on Ag (111) which may exist on the Ag (111) catalyst during the oxidation. However, a detailed analysis of the catalytic reaction as a function of the Cl adlayer phases should be explored further.

In the case of the bromide solution, the broad peak at -0.8 V in the voltammogram (Fig. 3b) might be due to Br anion adsorption, which is obviously not well ordered. It apparently rearranges into the $\sqrt{3}$ superstructure at the more positive potential of $+0.1$ V, but is not uniformly distributed over the electrode surface because its intensity is weaker than the intensity of the substrate spots. These patterns differ from the simple $(\sqrt{3} \times \sqrt{3})R30°$ structure, as reported by Salaita et al. [4] and Goddard et al. [17], obtained from bromine vapour adsorption on Ag (111) which shows a LEED pattern with rather broad spots, indicating a weakly ordered Br adlayer. However, the LEED pattern in Fig. 8a showing splitting of the $(\sqrt{3} \times \sqrt{3})R30°$ pattern is similar to that reported by Holmes et al. [18] obtained from Br gas phase adsorption under UHV conditions, except for the different orientation of the triangular spots and the absent extra spots which lie around the substrate spots as shown in ref. 18. Holmes et al. interpreted their LEED pattern in terms of a compression structure of a $(\sqrt{3} \times \sqrt{3})R30°$-Br with an ordered incommensurate phase. Indeed, the second-order extra spots of an incommensurate $(\sqrt{3} \times \sqrt{3})R30°$ structure should lie around the substrate beams which are drawn in the schematic pattern of their paper [18]. On the contrary, no additional reflection around the substrate beams can be seen in either the LEED or the RHEED patterns of the present work; a possible explanation for the splitting of the fractional-order beams may be given in terms of the scattering of the antiphase domains of the $(\sqrt{3} \times \sqrt{3})R30°$-Br adlayer; the Br adatoms form locally an ordered $(\sqrt{3} \times \sqrt{3})R30°$ structure with a mean domain size of 20 Å whose dimension is obviously defined by the Gibbs energy of the Br adlayer phase. These $\sqrt{3}$ patches arrange statistically with each other to give an antiphase domain structure which gives rise to a global (10×10) structure as shown in Fig. 9. The model of this surface structure successfully reproduces the observed diffraction patterns shown in Fig. 8. The Br coverage deduced from this model is about 1/3 monolayer. The coulometric estimated Br charge density from the curve of Fig. 3b is of the order of 100 μC/cm, which is very close to the value obtained by Schmidt and Stucki [19]. This value with the Br coverage (1/3 monolayer) deduced from the diffraction patterns (Fig. 8) gives a value of 0.6 for the electrosorption valency of Br.

It is interesting to note that under UHV conditions, only a diffuse $(\sqrt{3} \times \sqrt{3})R30°$ pattern could be seen at room temperature at the submonolayer coverage [17,18], while at low temperature ($\simeq 240$ K), it was transformed into an incommensurate $(\sqrt{3} \times \sqrt{3})R30°$-Br ordered phase with a Br–Br separation of 4.1–4.4 Å, which is about 11–17% smaller than that of a $(\sqrt{3} \times \sqrt{3})R30°$ structure [18]. On the other hand, when the Ag (111) electrode is emersed at 0.1 V, the Br adatoms even form a commensurate $\sqrt{3}$ structure at room temperature. Its ordering seems to be dependent on the surroundings.

The present work demonstrates that RHEED can observe not only any kind of surface structure, but also a surface structure consisting of a few layers. Besides its

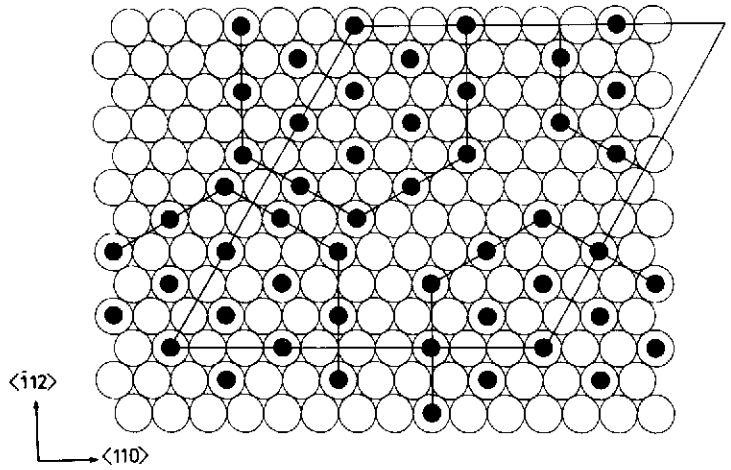

Fig. 9. Model of the surface structure of antiphase domains of the $(\sqrt{3} \times \sqrt{3})$R30°-Br structure on the Ag (111) substrate surface.

higher resolution compared with LEED, it can also observe surface roughness (facetting) and can be used to measure Auger spectra during the RHEED observation. The advantages of RHEED over LEED have been reported by Kolb et al. [8] and Ino [20].

CONCLUSIONS

(a) No ordered halide layer is observed from the emersed Ag electrode at very negative potentials around -0.9 V, except for the salt crystals of NaCl and NaBr due to wet emersion, which can be identified only by RHEED.

(b) Cl adatoms form a random layer at low Cl coverage, when the Ag electrode is emersed below $+0.1$ V, but an ordered (1.38×1.38) overlayer with higher Cl coverage is obtained when the electrode is emersed from the chloride solution around $+0.15$ V. This Cl adlayer forms obviously, with the topmost Ag layer, an AgCl layer. Thus, the anodic peak around 0.0 V may represent a phase transition of the Cl adatoms from an amorphous to an ordered overlayer.

(c) Ordered adsorption of Br on the Ag (111) surface occurs only at a potential between 0.0 and $+0.1$ V, showing a global (10×10) structure which is combined with a local $(\sqrt{3} \times \sqrt{3})$ R30°-Br structure. The anodic peak around 0 V may indicate a phase transition as in the case of Cl. However, no three-dimensional growth of AgBr on the Ag electrode surface was observed.

(d) The electrosorption valency of Cl and Br anions on an Ag electrode is of the order of 1 and 0.6, respectively.

ACKNOWLEDGEMENTS

I wish to thank Professor D.M. Kolb, Dr. G. Lehmpfuhl and Dr. D. Weick for helpful discussions and for a critical review of the manuscript. I also extend my thanks to the collaboration with the Laboratory for Catalysis, Dalian Institute of Chemical Physics, China for supplying data on the Cl gas phase adsorption.

REFERENCES

1 A. Bewick and B. Thomas, J. Electroanal. Chem., 84 (1977) 127.
2 G. Valette, A. Hamelin and R. Parsons, Z. Phys. Chem., N.F., 113 (1978) 71.
3 G. Valette and R. Parsons, J. Electroanal. Chem., 204 (1986) 291.
4 G.N. Salaita, F. Lu, L.L. Davidson and A.T. Hubbard, J. Electroanal. Chem., 229 (1987) 1.
5 Zhai Runsheng, Deng Junzhuo, Gao Yuming, Wei Xuming, Guo Xiexian and M.S. Zei, Surf. Sci., in press.
6 M.S. Zei, G. Qiao, G. Lehmpfuhl and D.M. Kolb, Ber. Bunsenges. Phys. Chem., 91 (1987) 349.
7 M.S. Zei, G. Lehmpfuhl and D.M. Kolb, Surf. Sci., 221 (1989) 156.
8 D.M. Kolb, G. Lehmpfuhl and M.S. Zei, NATO–ASI Series C, Spectroscopic and Diffraction Techniques in Interfacial Electrochemistry, Kluwer, 1990, pp. 361–382.
9 G. Comsa, Surf. Sci., 81 (1979) 57.
10 M. Bowker and K.C. Waugh, Surf. Sci., 134 (1983) 639.
11 Y. Tu and J.M. Blakely, J. Vac. Sci. Technol., 15 (1978) 563.
12 E. Batels and A. Goldmann, Solid State Commun., 44 (1982) 1419.
13 S.P. Weeks and J.E. Rowe, J. Vac. Sci. Technol., 16 (1979) 470.
14 W. Sesslmann and T.J. Chuang, Surf. Sci., 184 (1987) 374.
15 H.H. Voqe and C.R. Adams, Adv. Catal., 17 (1967) 151.
16 G. Rovida, F. Pratezi and E. Ferroni, J. Catal., 41 (1976) 140.
17 P.J. Goddard, K. Schwaha and R.M. Lambert, Surf. Sci., 71 (1978) 351.
18 D.J. Holmes, N. Panagiotides and D.A. King, Surf. Sci., 222 (1989) 285.
19 E. Schmidt and S. Stucki, Ber. Bunsenges. Phys. Chem., 77 (1973) 913.
20 S. Ino, J. Appl. Phys. Jpn, 16 (1977) 891.